Fish & Shellfish Immunology 35 (2013) 1455–1465

Contents lists available at ScienceDirect

Fish & Shellfish Immunology

journal homepage: www.elsevier.com/locate/fsi

Full length article

A teleostean counterpart of ferritin M subunit from rock bream (*Oplegnathus fasciatus*): An active constituent in iron chelation and DNA protection against oxidative damage, with a modulated expression upon pathogen stress

Don Anushka Sandaruwan Elvitigala [a], H.K.A. Premachandra [a], Ilson Whang [a,*], Myung-Joo Oh [b], Sung-Ju Jung [b], Choul-Ji Park [c], Jehee Lee [a,d,*]

[a] Department of Marine Life Sciences, School of Marine Biomedical Sciences, Jeju National University, Jeju Self-Governing Province 690-756, Republic of Korea
[b] Department of Aqualife Medicine, Chonnam National University, Chonnam 550-749, Republic of Korea
[c] Genetics & Breeding Research Center, National Fisheries Research & Development Institute, Geoje 656-842, Republic of Korea
[d] Marine and Environmental Institute, Jeju National University, Jeju Special Self-Governing Province 690-814, Republic of Korea

ARTICLE INFO

Article history:
Received 9 May 2013
Received in revised form
8 August 2013
Accepted 14 August 2013
Available online 24 August 2013

Keywords:
Ferritin M
Rock bream
Iron chelation
DNA protection effect
Transcriptional analysis

ABSTRACT

Ferritins are biological iron chelators that can sequestrate excess iron to maintain iron homeostasis in the body. Ferritins basically consist of 2 types of subunits, designated as H and L. However, another new subunit, ferritin "M" which possesses characteristic features of both the H and L subunits, was recently identified in lower vertebrates, mostly in fish. In this study, a ferritin M-like subunit from rock bream (*Oplegnathus fasciatus*) (RbFerM) was characterized at the molecular level, and its transcriptional profile was analyzed in healthy fish, as well as in pathogen- and mitogen-stimulated fish. Furthermore, its functional properties were evaluated using the recombinant protein. The complete coding sequence of RbFerM was 528 bp in length, encoding a 176-amino acid peptide with a calculated molecular mass of 20 kDa. *In silico* analysis of RbFerM revealed that it has features similar to both the mammalian ferritin subunits, H and L. Phylogenetic analysis depicted the higher evolutionary proximity of RbFerM with its fish counterparts. Quantitative real time polymerase chain reaction (PCR) analysis detected a ubiquitous transcriptional profile of RbFerM in selected tissues of rock bream, in which more pronounced expression was observed in blood and liver tissues. Significant transcriptional inductions of RbFerM were detected in liver tissues upon lipopolysaccharides (LPS), *Edwardsiella tarda*, *Streptococcus iniae*, and rock bream irido virus (RBIV) exposures in time-course immune-challenge experiments. The purified recombinant protein of RbFerM demonstrated detectable iron chelating activity that varied with the temperature. Moreover, the recombinant RbFerM rendered a detectable protection effect against iron (II) and H_2O_2-mediated DNA damage.

1. Introduction

Iron is known to be an essential trace element because it is involved in several crucial biological processes of living organisms. However, excess iron levels in cellular environments cause deleterious effects, as iron can catalyze the production of reactive oxygen species in cells, thereby resulting in oxidative stress [1]. Therefore, maintaining an iron balance is considered essential for an organism's survival. In this regard, ferritins play an important role in iron homeostasis in the body while sequestrating excess iron and releasing them in iron dearth [2].

Ferritin is a ubiquitous and highly conserved hollow spherical protein complex comprising 24 subunits, and it is capable of mineralizing approximately 4500 iron atoms inside its thick protein shell [3]. These subunits that assemble into ferritin are composed of 2 basic types of polypeptide chains, designated as H and L [4], which are encoded by 2 distinct genes [5,6]. The H

* Corresponding authors. Marine Molecular Genetics Lab, Department of Marine Life Sciences, College of Ocean Science, Jeju National University, 66 Jejudaehakno, Ara-Dong, Jeju 690-756, Republic of Korea. Tel.: +82 64 754 3472; fax: +82 64 756 3493.
E-mail addresses: ilsonwhang@hanmail.net (I. Whang), jehee@jejunu.ac.kr, jeheedaum@hanmail.net (J. Lee).

1050-4648/$ – see front matter © 2013 Elsevier Ltd. All rights reserved.
http://dx.doi.org/10.1016/j.fsi.2013.08.012

subunits consist of catalytic iron-binding sites, which form the ferroxidase center [7], whereas L subunits bear negatively charged amino acid residues known as iron nucleation sites, which provide ligands for binding Fe^{3+} ions [8]. The proportion of H and L subunits in the ferritin protein complex can greatly vary depending on the tissue type and physiological status of the cell. L subunits are predominantly found in ferritins of liver and spleen tissues, whereas H subunits are mainly found in ferritins of the heart and kidney [9]. Ferritin recognizes and binds Fe^{2+} ions in the ferroxidase center, where Fe^{2+} ions are oxidized by di-oxygen to Fe^{3+} [10]. Subsequently, Fe^{3+} binds to the nucleation sites of the L subunit for mineralization [8]. However, H-rich ferritins are known to be more active in iron metabolism than L-rich ferritins [7]. Moreover, in order to protect DNA from iron toxicity, H ferritins can translocate to the nuclei in some cell types or can be actively secreted to exert a wide array of biological functions [4].

Recent studies have revealed a novel subunit of the ferritin complex known as M, which is encoded by a single distinct gene and possesses active sites characteristic of both H and L subunits. The ferritin M subunit has been identified in lower vertebrate lineages, including piscines [4,11–13]. Ferritins are abundantly found in their cytosolic form; however, they can also be encountered in mammalian mitochondria and in the nuclei of plant plastids, as well as in their secreted forms in insects [4].

Recent investigations on the function of ferritin have revealed its multiple roles in organisms apart from iron homeostasis. Ferritins have also been shown to be involved in cell activation, development, immunity, and angiogenesis in animals [14–17], while orchestrating the cellular defense mechanisms against stress and inflammation [18].

Ferritin expression is regulated at both the transcriptional and posttranscriptional levels by iron response proteins, which control the amount of the protein that is expressed in or is secreted from cells [19–21]. Ferritin transcription can be modulated by different external factors such as iron flux [22], pathogen infections [13], xenobiotic stress [19], pH stress [23], and temperature [24], as well as internal factors such as oxidative stress [13], inflammatory cytokines, oncogenes, growth factors, and second messengers [19].

Ferritins can be found in a wide array of organisms from microorganisms to higher vertebrates, as well as in plants [25]. Its basic subunits, H and L, have previously been characterized from various animals, including fish. The ferritin M subunit has been identified and characterized from several marine teleost species, including *Cynoglossus semilaevis* [26], *Pseudosciaena crocea* [27], *Sciaenops ocellatus* [28], *Scophthalmus maximus* [13], and *Salmo salar* [11].

Rock bream (*Oplegnathus fasciatus*) is an economically important delicacy that is harvested by commercial fisheries and mariculture farming, accounting for prominent fish yields in eastern and southeastern Asia. However, various environmental factors can affect its growth and survival, some of which have even resulted in the reduction of mariculture production. Pathogen infections, especially bacterial and viral attacks, play a key role in such reductions by causing oxidative stress in fish, thereby affirming the necessity of a precise disease management strategy to ensure sustainability in fish mariculture farming [29,30]. In this regard, investigations of immune and oxidative defense mechanisms in this aqua-crop have become an effective approach for developing appropriate preventive schemes.

Herein, we identified and characterized a teleostean counterpart of the ferritin M subunit (RbFerM) from rock bream (*O. fasciatus*) and analyzed its transcriptional modulation upon pathogen infection. Furthermore, the iron chelating activity of purified recombinant RbFerM was demonstrated under different protein concentrations and temperatures, further evaluating its potent DNA protection effects against oxidative damage.

2. Materials and methods

2.1. Identification and sequence profiling

The complete cDNA sequence of RbFerM was identified from our sequence database of the previously constructed rock bream cDNA library [31] using the Basic Local Alignment Tool (BLAST) algorithm (http://blast.ncbi.nlm.nih.gov/Blast.cgi). Subsequently, the identified sequence was characterized using different bioinformatics tools. Prediction of protein domains was carried out using the ExPASy-prosite database (http://prosite.expasy.org) and the MotifScan scanning algorithm (http://myhits.isb-sib.ch/cgi-bin/motif_scan), whereas other properties of RbFerM were determined using the ExPASy Prot-Param tool (http://web.expasy.org/protparam). Pairwise sequence alignment and multiple sequence alignment with orthologous sequences were performed using the EMBOSS needle program (http://www.Ebi.ac.uk/Tools/emboss/align) and the ClustalW2 program (http://www.Ebi.ac.uk/Tools/clustalw2), respectively. The phylogenetic relationship of RbFerM was determined using the neighbor-joining method and the Molecular Evolutionary Genetics Analysis (MEGA) software version 4 [32]. The reliability of the resultant phylogenetic reconstruction was tested using 1000 bootstrap replications.

2.2. Overexpression and purification of the recombinant RbFerM fusion protein

Recombinant RbFerM was expressed as a fusion protein with the maltose binding protein (MBP), and purified as described previously [33], with some modifications. Briefly, the coding sequence of the RbFerM gene was amplified using the sequence-specific primers RbFer-F and RbFer-R, which contained restriction enzyme sites for *Eco*RI and *Hin*dIII, respectively (Table 1). Polymerase chain reaction (PCR) was performed in a TaKaRa thermal cycler in a total volume of 50 μL with 5 U of ExTaq polymerase (TaKaRa, Japan), 5 μL of 10× ExTaq buffer, 8 μL of 2.5 mM dNTPs, 80 ng of template, and 20 pmol of each primer. The reaction was carried out at 94 °C for 30 s, 55 °C for 30 s, 72 °C for 1 min, followed by a final extension at 72 °C for 5 min. The PCR product (~530 bp) was resolved in 1%

Table 1
Oligomers used in this study.

Name	Purpose	Sequence (5′ → 3′)
RbFerM-qF	BAC library screening and q-PCR of *RbFerM*	TCAACATGGAGCTGTTTGCCTCTTACT
RbFerM-qR	BAC library screening and q-PCR of *RbFerM*	ACAACTTCAGAGCTGACATCAGCTTCT
RbFerM-F	ORF amplification (*Eco*RI)	GAGAGAgaattcATGGAGTCCCAAGTGCGTCAG
RbFerM-R	ORF amplification (*Hin*dIII)	GAGAGAaagcttTTAGCT CTT GCC CCC CAGG
Rb-βF	q-PCR for rock bream β-actin gene	TCATCACCATCGGCAATGAGAGGT
Rb-βR	q-PCR for rock bream β-actin gene	TGATGCTGTTGTAGGTGGTCTCGT

agarose gel, excised, and purified using the Accuprep™ gel purification kit (Bioneer Co., Korea). The digested pMAL-c2X vector (150 ng) and the PCR product (60 ng) were ligated using Mighty Mix (7.5 μL; TaKaRa) at 4 °C overnight. The ligated pMAL-c2X/RbFerM product was transformed into DH5α cells and sequenced. After sequence confirmation, the recombinant expression plasmid was transformed into *Escherichia coli* BL21 (DE3) competent cells. The recombinant RbFerM protein was then overexpressed using isopropyl-β-D-galactopyranoside (IPTG, 1 mM final concentration) induction in *E. coli* cells, grown in a 500 mL Luria broth (LB) medium supplemented with ampicillin (100 μg/mL) and glucose (0.2% final concentration) at 37 °C for 3 h. After the incubation at 37 °C, induced *E. coli* BL21 (DE3) cells were cooled on ice for 30 min and harvested by centrifugation at 3500 rpm for 30 min at 4 °C. Harvested cells were resuspended in 20 mL of column buffer (20 mM Tris–HCL, pH 7.4, 200 mM NaCl) and stored at −20 °C. Subsequently, the protein was purified using the pMAL™ protein fusion and purification system (New England Biolabs, Ipswich, MA). Briefly, the cells were thawed in an ice water bath and lysed by cold sonication. The lysate was then centrifuged at 13,000 × *g* for 30 min at 4 °C and resultant supernatant (crude extract) was subsequently mixed with I mL of amylose resin and placed on ice for 2 h while mixing within every 10 min to facilitate affinity binding. Thereafter, the settled resin-extract mixture was loaded onto a 1 cm × 5 cm column and washed with 12× volume of the column buffer. Finally, the rRbFerM–MBP fusion protein was eluted using an elution buffer (10 mM maltose), and its concentration was determined by the Bradford method by using bovine serum albumin as the standard [34]. Next, the recombinant RbFerM–MBP fusion product was cleaved using factor Xa, according to the pMAL™ protein fusion and purification protocol (New England Biolabs, Ipswich, MA). The resultant non-fused RbFerM (rRbFerM) was assayed for its iron chelation and DNA protection activities. The RbFerM samples that were collected at different purification steps followed by cleavage with factor Xa were analyzed by 12% sodium dodecyl sulfate polyacrylamide gel electrophoresis (SDS-PAGE) under reduced conditions by using standard protein size markers (Enzynomics, Korea). The gel was stained with 0.05% Coomassie blue R-250, followed by a standard de-staining procedure.

2.3. Effect of rRbFerM protein concentration on the iron chelating activity

The iron chelating activity of rRbFerM was determined using a previously published method with some modifications [35]. Briefly, 20 μL of 2 mM $FeSO_4$ was added to different concentrations of the recombinant protein in 1 mL of column buffer (20 mM Tris–HCl and 200 mM NaCl) and was incubated at room temperature (27 °C) for 10 min. Thereafter, 5 mM ferrozine (Sigma, USA) was added to each mixture, mixed thoroughly, and then incubated again at the same temperature for 15 min. Finally, the optical density (OD) of each mixture was measured using a spectrophotometer at 562 nm. Corresponding concentrations of MBP were used as controls in each assay to investigate the effect of MBP in the cleaved recombinant fusion protein sample. Each assay was performed in triplicate, and the mean OD value was used for the calculation of the percentage iron (II) chelation.

2.4. Effect of temperature on the iron chelation activity of rRbFerM

The iron chelating activity of rRbFerM was measured at increasing temperatures by using 50 μg/mL of the recombinant protein. The methods described in Section 2.3 were followed, except that the temperature of first incubation was changed. Each assay proceeded in parallel with factor Xa-treated MBP and equal volume of elusion buffer, instead of the recombinant protein, as controls. Assays were performed in triplicate to obtain the mean OD_{562} value. This mean value was used in the final calculation of the percentage of chelated Fe (II) ions: (OD_{562} of the negative control − OD_{562} of the assay mixture/OD_{562} of the negative control) × 100.

2.5. Determination of the DNA protection effect of rRbFerM under oxidative stress

In order to investigate the DNA protection activity of rRbFerM from strand breakage under oxidative stress, the conversion of supercoiled plasmid DNA to nicked circular form DNA was measured with and without the addition of rRbFerM in the reaction mixture of iron (II) ions and H_2O_2, as previously described [36], with some modifications. Briefly, rRbFerM was added to the iron (II) solutions (0.4 mM) in column buffer to achieve final concentrations of 0.5, 1, and 2 μg/μL in a total volume of 45 μL and the mixtures were then incubated at 37 °C for 15 min. Subsequently, the mixtures were treated with pUC19 (2 μg) and H_2O_2 (final concentration of 4 mM in the reaction mixture). Mixtures were incubated at 37 °C for 15 min in order to elicit DNA breakage through the formation of hydroxyl radicals from the reaction of iron (II) and H_2O_2. A factor Xa-treated MBP (at a final concentration of 2 μg/μL) assay was conducted in parallel without the addition of rRbFerM as a control. Immediately after incubation, DNA in each reaction mixture was purified separately by using the AccuPrep® PCR purification kit (Bioneer, Korea) according to manufacturer's instructions, thus terminating the DNA cleavage reactions. Thereafter, the purified DNA was eluted into 25 μL of DNA elution buffer, and the total volume was loaded and analyzed by electrophoresis on 1% agarose gel with undigested, pure pUC19 vector DNA to observe the respective bands.

2.6. Experimental fish and tissue collection

Healthy Rock bream with an average body weight of 50 g were obtained from the Jeju Special Self-Governing Province Ocean and Fisheries Research Institute (Jeju, Republic of Korea). Animals acclimatized for 1 week prior to the experiment in a controlled environment (salinity 34 ± 1 psu, pH 7.6 ± 0.5, at 22–24 °C) in 400 L tanks and fed with commercially available fish feed were used for tissue collection. Whole blood (1 mL/fish) was collected from the caudal fin by using a sterilized syringe, and the sample was immediately centrifuged at 3000 × *g* for 10 min at 4 °C to separate the blood cells from the plasma. The collected cells were snap-frozen in liquid nitrogen. Meanwhile, the sampled fish was sacrificed, and the gill, liver, skin, spleen, head kidney, kidney, heart, muscle, brain, and intestine were excised, which were immediately snap-frozen in liquid nitrogen and stored at −80 °C until use for total RNA extraction.

2.7. Immune-challenge experiments

In order to determine the transcriptional modulation of RbFerM upon pathogen infections, *Streptococcus iniae*, *Edwardsiella tarda*, rock bream iridovirus (RBIV), and lipopolysaccharides (LPS) served as immune-stimulants in time-course immune-challenge experiments. Two bacterial pathogens were obtained from the Department of Aqualife Medicine, Chonnam National University, Korea. The bacteria were incubated at 25 °C for 12 h using a brain heart infusion (BHI) broth (Eiken Chemical Co., Japan) supplemented with 1% sodium chloride. The cultures were resuspended in sterile phosphate-buffered saline (PBS) and subsequently diluted to a desired concentration to inject fish. For the virus challenge experiment, kidney tissue specimens obtained from the moribund rock

bream infected with RBIV were homogenized in 20 volumes of PBS and then centrifuged at 3000 × *g* for 10 min at 4 °C to obtain the supernatant of RBIV sample. Subsequently, the obtained supernatant was filtered through a 0.45 μm membrane and used to inject fish. The immune-challenge experiments were carried out as previously described, sacrificing at least 3 animals for tissue collection from each challenge group at each time point [37]. Thereafter, tissues were collected as described in Section 2.6.

2.8. Total RNA extraction and cDNA synthesis

Total RNA was extracted by Tri Reagent™ (Sigma – USA) from blood, gill, liver, spleen, head kidney, kidney, skin, muscle, intestine, and brain tissues from healthy rock breams, as well as from liver tissues collected from immune-challenged animals. Subsequently, cDNAs were synthesized from each set of RNA, as previously described [31].

2.9. RbFerM transcriptional analysis by quantitative real time PCR (q-PCR)

q-PCR was used to analyze the expression levels of RbFerM in blood, gill, liver, spleen, head kidney, kidney, skin, muscle, brain, and intestine tissues of healthy fish, and the temporal expression of RbFerM in liver tissues of immune-challenged animals. Total RNA was extracted at different time points following the

```
                                                GACACCAGGG AAGAAAACCTTAAGG AGTTCTTGCTTCAAC AGTGTTTGAACGGAA -205

CTTCTTCCTTCGTCC CGCTTTGTTTATCAA CTAATCTGCATTCCG GAAGACGAACAACCT TTTTCTAATTGAACA -150

CTACTGATAAAGTCG TCGTGAAGCTCTATT TTTGTACCGTTTTGT TAAAGAAAAGCACAA GAACCGCCAGCCAAG  -75

ATGGAGTCCCAAGTG CGTCAGAACTACCAC CGCGACTGCGAGGCC GCCATCAACCGAATG GTCAACATGGAGCTG   75

  M  E  S  Q  V  R  Q  N  Y  H  R  D  C  E  A  A  I  N  R  M  V  N  M  E  L   25

TTTGCCTCTTACTCC TACACTTCAATGGCC TTTTACTTCTCCCGT GACGATGTGGCCCTT CCAGGCTTCTCCCAT  150

  F  A  S  Y  S  Y  T  S  M  A  F  Y  F  S  R  D  D  V  A  L  P  G  F  S  H   50

TTCTTCAAGGAGAAC AGCGAGGAGGAGAGG GAGCACGCCGAGAAG CTGCTGTCCTTCCAG AACAAAAGAGGAGGA  225

  F  F  K  E  N  S  E  E  E  R  E  H  A  E  K  L  L  S  F  Q  N  K  R  G  G   75

CGCATCTTCCTCCAG GACATCAAGAAACCG GAGCGTGATGAGTGG GGGAGTGGGCTGGAG GCCATGCAGTGCGCC  300

  R  I  F  L  Q  D  I  K  K  P  E  R  D  E  W  G  S  G  L  E  A  M  Q  C  A  100

CTGCAGCTGGAGAAG AACGTCAACCAGGCT CTGCTGGACCTGCAC AAACTGGCCTCCGAG CACGGAGACCCTCAT  375

  L  Q  L  E  K  N  V  N  Q  A  L  L  D  L  H  K  L  A  S  E  H  G  D  P  H  125

CTGTGTGACTTCCTG GAGACCCACTACCTG AACGAGCAGGTGGAG GCCATCAAGAAGCTG GGCGACTACATTTCC  450

  L  C  D  F  L  E  T  H  Y  L  N  E  Q  V  E  A  I  K  K  L  G  D  Y  I  S  150

AACCTCAGCCGCATG GACGCCCACACCAAC AAGATGGCGGAGTAC CTGTTTGACAAGCAT TCCCTGGGGGGCAAG  525

  N  L  S  R  M  D  A  H  T  N  K  M  A  E  Y  L  F  D  K  H  S  L  G  G  K  175

AGCTAAACGCAAAGT CCCATGATGGAGCCT GGAGTGAAAATCTTA ATGACACACAGGCTT TAAACTAAACACGCG  600

  S

TTTCTGCTTTGGCTG CTCATTCACTGAGCG CAATATATCTAATCT GCTTAACCTATGAAG TTGACAAGTTCTGGT  675
ATGTCGTGGTGGTGT CGCTGTTTTTAAATG TCATATGGAAGGATG GATATTAATCAGGTT ACGGCTTTGCCCTCA  750
TTACCTATAAGCCTC CTTGTGACATTTTTA ACAATGATTGTGACT GAATGTTTCTGATCT GTTCTTAATCTGAAT  825
AAACATTTTTGAGCT AGGAAAAAAAA                                                       851
```

Fig. 1. Nucleotides and deduced amino acid sequence of RbFerM. Start codon (ATG), stop codon (TAA), and poly A signal (AATAA) are underlined. The iron response element (IRE) at the 5′ UTR is underlined, and the 2 putative iron-binding region signatures (IBRS) are depicted with gray shading. Seven metal ligands responsible for iron binding and ferroxidation are shown in boxes, whereas residues involved in iron nucleation are represented in red color font. (For interpretation of the references to color in this figure legend, the reader is referred to the web version of this article.)

respective immune challenges, and first-strand cDNA synthesis was carried out as described in Section 2.8. q-PCR was carried out using the thermal cycler Dice™ Real Time System (TP800; TaKaRa, Japan) in a 15 μL reaction volume containing 4 μL of diluted cDNA from each tissue, 7.5 μL of 2× TaKaRa ExTaq™ SYBR premix, 0.6 μL of each primer (RbFer-qF and RbFer-qR; Table 1), and 2.3 μL of ddH_2O. q-PCR analysis was performed under the following conditions: 95 °C for 10 s, followed by 35 cycles of 95 °C for 5 s, 58 °C for 10 s, and 72 °C for 20 s, and a final cycle of 95 °C for 15 s, 60 °C for 30 s, and 95 °C for 15 s. The baseline was set automatically by Dice™ Real Time System software (version 2.00). Moreover, no template control experiments were carried out to affirm that the PCR reagents were not contaminated with templates. Since we have designed the q-PCR oligomers flanking two exon-intron boundaries, affirmed by two different sized bands (~200 bp with respect to cDNA template and ~700 bp with respect to genomic DNA template) observed in agarose gel electrophoresis after the PCR amplification of the target DNA fragments using both synthesized cDNA and genomic DNA as templates, undetectable effect of potential genomic DNA contamination in total RNA samples was ascertained by the signal peaked melting curves of the amplicon of each q-PCR experiment. In order to confirm the specific amplification of the target using respective oligomers, corresponding melting curve analysis was carried out and product size (~200 bp) was affirmed by agarose gel electrophoresis. RbFerM expression was determined by the Livak ($2^{-\Delta\Delta CT}$) method [38]. The same q-PCR cycle profile was used for the internal control gene, rock bream β-actin (GenBank ID: FJ975145) by using respective oligomers (Table 1), which did not show any significant expressional variation within each tissue under provided experimental conditions. All data are presented as means ± standard deviation (SD) of the relative mRNA expression of 3 replicates. To determine statistical significance ($P < 0.05$) between the experimental and control groups, two-tailed unpaired student *t*-tests were carried out. In all q-PCR analyses regarding immune challenge experiments, expression levels of RbFerM mRNA relative to the corresponding fold-change in expression of the rock bream β-actin gene were detected, and these were further normalized to the corresponding phosphate-buffered saline (PBS)-injected controls at each time point. The relative expression level at the 0-h time point (uninjected control) was used as the baseline reference.

3. Results and discussion

3.1. Sequence characterization of RbFerM

The complete cDNA sequence of RbFerM was consisted of 1056 bp, in which the coding sequence comprised 528 bp, whereas the 5′ and 3′ untranslated region (UTR) sequences contained 205 and 323 bp, respectively. Interestingly, a regulatory element that modulates ferritin expression upon iron load, designated as the iron response element (IRE) [39], was identified within the 5′ UTR of the RbFerM cDNA sequence (Fig. 1). With respect to the predicted protein sequence, the molecular mass of RbFerM was determined to be approximately 20 kDa, and the theoretical isoelectric point was 5.58, as predicted by the ExPASy Prot-Param tool. Bioinformatics analysis revealed that RbFerM contained featured characteristics of both ferritin H and L subunits, affirming that the derived protein sequence was indeed an ortholog of the ferritin M subunit. Two ferritin iron-binding signatures (IBRS; residues 58–76 and 123–143), 7 metal ligands important in iron binding and ferroxidation in mammalian ferritin H subunits (E-24, Y-31, E-58, E-59, H-62, E-104, and Q-138), as well as residues involved in iron nucleation in the mammalian ferritin L subunit were identified in the deduced peptide sequence of RbFerM (Fig. 1).

Pairwise sequence alignment of RbFerM with its homologs reflected substantial compatibility with its vertebrate counterparts, especially with fish, and the highest percent identity (96.6%) and similarity (99.4%) was observed with the ferritin M subunit of the red drum, *S. ocellatus* (Table 2). Moreover, multiple sequence alignment demonstrated that the residues responsible for iron binding and ferroxidation in RbFerM were highly conserved among the ferritin H and M subunits of other vertebrates, whereas anticipated residues in the iron nucleation center showed conservation among ferritin L and M subunits of other vertebrate species, thereby validating our ferritin subunit as an ortholog of the M subunit (Fig. 2).

3.2. Evolutionary proximity of RbFerM with its orthologs

The phylogenetic analysis of RbFerM using different counterparts of ferritin subunits resulted a tree construct indicating three main clusters of ferritin subunits, M, H and L. As expected, members of respective fish and mammalian ferritin subunits were clustered closely and independently where ferritin M cluster represented exclusively a piscine origin, convincing its restricted distribution among lower vertebrates. It is also intriguing to note that the cluster of all ferritin M counterparts was supported by a prominent bootstrapping value (98) where RbFerM was clustered with a subgroup of red drum and large yellow croaker ferritin M subunits which was also supported by a fairly high bootstrapping value (71), reflecting a close evolutionary relationship with its teleostean counterparts (Fig. 3). In contrast, compared to ferritin M subunits, RbFerM showed a distant relationship with L and H subunits of vertebrate species, which formed separate clades with its orthologs, affirming its evolutionary deviation from H and L subunits. Therefore, these observations affirmed that RbFerM has evolved from a common ancestor indicating that it is indeed an ortholog of vertebrate ferritin M subunits.

3.3. Integrity and purity of overexpressed recombinant RbFerM (rRbFerM)

The SDS-PAGE analysis reflected the successful overexpression of rRbFerM in *E. coli* cells further revealing the significant purity and integrity of the finally eluted fusion product through the appearance of signal band on corresponding lane of the purified

Table 2
Percentage similarity and identity values of RbFerM and its orthologs.

Name	NCBI-GenBank accession no.	Amino acids	% Identity	% Similarity
1. *Sciaenops ocellatus* (red drum)	ADF80517	176	96.6	99.4
2. *Larimichthys crocea* (large yellow croaker)	ACY75476	176	95.5	99.4
3. *Scophthalmus maximus* (turbot)	ADI24354	176	92.6	97.7
4. *Anoplopoma fimbria* (sablefish)	ACQ57862	176	90.9	97.7
5. *Salmo salar* (Atlantic salmon)	ACI67714	176	88.1	96.6
6. *Oncorhynchus mykiss* (rainbow trout)	ACO08179	176	86.9	96.6
7. *Ictalurus punctatus* (catfish)	ADO29006	177	70.1	87.0
8. *Osmerus mordax* (rainbow smelt)	ACO09242	173	84.1	93.8

```
Human-H                 MTTASTS-QVRQNYHQDSEAAINRQINLELYASYVYLSMSYYFDRDDVALKNFAKYFLHQ 59
Mouse-H                 MTTASPS-QVRQNYHQDAEAAINRQINLELYASYVYLSMSCYFDRDDVALKNFAKYFLHQ 59
Catfish-H               ----MSS-QVRQNFHQDCEAAINRQINLELYASYVYLSMSYYFDRDDQALHNFAKFFRKQ 55
Atlantic salmon-M       ----MES-QIRQNYHHDCEAAINRMINMEMFASYTYTSMAFYFSRDDVALPGFAHFFKEN 55
Rainbow trout-M         ----MES-QIRQNYHHDCEAAINRMINLEMFASYTYTSMAFYFSRDDVALSGFAHFFKEN 55
Red drum-M              ----MES-QVRQNYHRDCEAAINRMVNMELFASYTYTSMAFYFSRDDVALPGFSHFFKEN 55
Large yellow croaker-M  ----MES-QVRQNYHRDCEAAINRMVNMELFASYTYTSMAFYFSRDDVALPGFSHFFKEN 55
Rock bream-M            ----MES-QVRQNYHRDCEAAINRMVNMELFASYSYTSMAFYFSRDDVALPGFSHFFKEN 55
Turbot-M                ----MES-QVRQNYNRDCEAAVNRMVNMELFASYTYTSMAFYFSRDDVALPGFSHFFKEN 55
Catfish-M               ----METSQIRQNYHRDCEAAINKMINMELYASYTYTSMAYYFTRDDVALEGFAHFFKEN 56
Mouse-L                 ----MTS-QIRQNYSTEVEAAVNRLVNLHLRASYTYLSLGFFFDRDDVALEGVGHFFREL 55
Human-L                 ----MSS-QIRQNYSTDVEAAVNSLVNLYLQASYTYLSLGFYFDRDDVALEGVSHFFREL 55
                              : *:***:  : ***:*  :*: : *** * *:. :* *** ** ...::* .

Human-H                 SHEEREHAEKLMKLQNQRGGRIFLQDIKEPDCDDWESGQNAMECALHLEKNVNQSLLELH 119
Mouse-H                 SHEEREHAEKLMKLQNQRGGRIFLQDIKKPDRDDWESGLNAMECALHLEKSVNQSLLELH 119
Catfish-H               SHEEREHAEKLMKVQNQRGGRIFLQDIKKPERDEWGSGMEALECALQLEKNVNQSLLDLH 115
Atlantic salmon-M       SEEEREHADKLLSFQNKRGGRILLQDIKKPERDEWGNGLEAMQCALQLEKNVNQALLDLH 115
Rainbow trout-M         SDEEREHADKLLSFQNKRGGRIFLQDIKKPERDEWGNGLEAMQCALQLEKNVNQALLDLH 115
Red drum-M              SDEEREHAQKLLSFQNKRGGRIFLQDVKKPERDEWGSGLEAMQCALQLEKNVNQALLDLH 115
Large yellow croaker-M  SDEEREHAQKLLSFQNKRGGRIFLQDVKKPERDEWGSGLEAMQCALQLEKNVNQALLDLH 115
Rock bream-M            SEEEREHAEKLLSFQNKRGGRIFLQDIKKPERDEWGSGLEAMQCALQLEKNVNQALLDLH 115
Turbot-M                SEEEREHADKLLSFQNNRGGRIFLQDVKKPEKDEWGSGLEAMQCALQLEKNVNQALLDLH 115
Catfish-M               SHEEREHAEKFMSFQNKRGGRIFLQDVKKPKRDEWGSGLEAMQCALQLEKTVNQALLDLH 116
Mouse-L                 AEEKREGAERLLEFQNDRGGRALFQDVQKPSQDEWGKTQEAMEAALAMEKNLNQALLDLH 115
Human-L                 AEEKREGYERLLKMQNQRGGRALFQDIKKPAEDEWGKTPDAMKAAMALEKKLNQALLDLH 115
                        :.*:**  :::::.**.**** ::**:::*  *:* .  :*::.*: :**.:**:**:**

Human-H                 KLATDKNDPHLCDFIETHYLNEQVKAIKELGDHVTNLRKMGAPE--------SGLAEYLF 171
Mouse-H                 KLATDKNDPHLCDFIETYYLSEQVKSIKELGDHVTNLRKMGAPE--------AGMAEYLF 171
Catfish-H               KVATDHNDPHMCDFIEAHYLDEQVKSIKELSDWVTNLRRMGAPQ--------NGMAEYLF 167
Atlantic salmon-M       KIASDKVDPHLCDFLETHYLNEQVEAIKKLGDHITNLTKMDAVK--------NKMAEYLF 167
Rainbow trout-M         KIASDKVDPHLCDFLETHYLNEQVEAIKKLGDHITNLTKMDAVK--------NKMAEYLF 167
Red drum-M              KLASEHVDPHLCDFLETHYLNEQVEAIKKLGDYISNLSRMDANT--------NKMAEYLF 167
Large Yellow croaker-M  KLASEHVDPHLCDFLESHYLNEQVEAIKKLGDYISNLTRMDAHT--------NKMAEYLF 167
Rock bream-M            KLASEHGDPHLCDFLETHYLNEQVEAIKKLGDYISNLSRMDAHT--------NKMAEYLF 167
Turbot-M                KLASDHVDPHMCDFLETHYLNEQVEAIKKLGDYISNLTRMDAKN--------NKMAEYLF 167
Catfish-M               KLASDKADPHLCDFLETHYLNEQVEAIKKLGDHISNLTKMDAAS--------NRMAEYLF 168
Mouse-L                 ALGSARADPHLCDFLESHYLDKEVKLIKKMGNHLTNLRRVAGPQPAQTGAPQGSLGEYLF 175
Human-L                 ALGSARTDPHLCDFLETHFLDEEVKLIKKMGDHLTNLHRLGGPE--------AGLGEYLF 167
                         :.: : ***:***:*:::*.::*: **::.: ::** :: .            :.****

Human-H                 DKHTLGDSDNES 183
Mouse-H                 DKHTLGHGD-ES 182
Catfish-H               DKHTLGSES--S 177
Atlantic salmon-M       DKHTLGGQS--- 176
Rainbow trout-M         DKHTLGGQS--- 176
Red drum-M              DKHSLGGKS--- 176
Large yellow croaker-M  DKHTLGGKS--- 176
Rock bream-M            DKHSLGGKS--- 176
Turbot-M                DKHSLGGKS--- 176
Catfish-M               DKHTLGGKS--- 177
Mouse-L                 ERLTLKHD---- 183
Human-L                 ERLTLKHD---- 175
                        :: :*
```

Fig. 2. Multiple sequence alignment of different vertebrate ferritin subunits. Sequence alignments were obtained using the ClustalW method. Conserved residues important in metal binding and ferroxidation among H and M subunits are shaded in gray, whereas residues involved in iron nucleation, showing high conservation among different M and L subunits, are indicated by green shading. (For interpretation of the references to color in this figure legend, the reader is referred to the web version of this article.)

recombinant fusion protein (Fig. 4). Moreover, the molecular mass of the protein was observed to be approximately 60 kDa, which conformed to the molecular mass of the predicted RbFerM (~20 kDa), because the molecular mass of MBP is ~42.5 kDa. In addition, the products obtained after cleavage of the fusion protein resolved as 2 bands, affirming the complete cleavage of the rRbFerM–MBP fusion product into MBP and rRbFerM, as evident by the corresponding band sizes in the gel.

3.4. Iron chelation activity of different concentrations of rRbFerM

The iron chelation activity of the rRbFerM protein was demonstrated using an assay system based on the OD reduction of the iron (II)-ferrozine chromogenic complex at 562 nm, which occurs upon binding of Fe (II) ions by ferritin. As shown in Fig. 5, even under the lowest concentration of rRbFerM (0.006 μg/μL), percentage iron chelation was found to be significantly high, compared to the

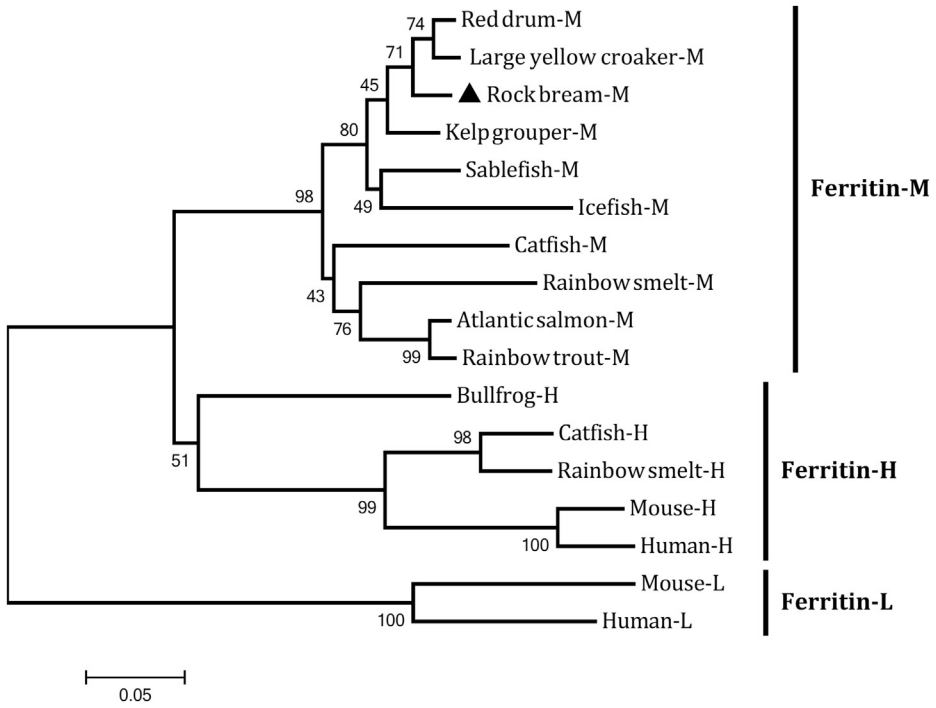

Fig. 3. Phylogenetic relationship of RbFerM and its orthologs. Evolutionary proximity of different ferritin subunits of their vertebrate counterparts was analyzed on the basis of ClustalW alignments of the respective protein sequences by using the neighbor-joining method of MEGA 4.0 software. Corresponding bootstrap values are indicated on the lineages of the tree. NCBI-GenBank accession numbers of the protein sequences of ferritin M subunits are listed in Table 1 except icefish (CCO75659) and kelp grouper (AEI87383). Gen Bank accession numbers for H and L ferritin subunits are as follows: Bullfrog-H: AAA49532, catfish-H: NP001187267, rainbow smelt-H: ACO09727, mouse-H: AAH12314, human-H: AAH66341, mouse-L: NP034370, and human-L: AAA52439.

control (without the protein), further validating its structural predictions and similarities with the known ferritin M and H subunits of other species. However, subsequent increases of rRbFerM concentration resulted in stable iron binding of rRbFerM, as evidenced by the plateau shape of the curve (Fig. 5). Furthermore, the initial protein concentration (0.012 μg/μL) of the plateau may also represent the optimal concentrations for iron chelation at the given conditions. The control experiment with MBP did not show any significant iron chelation at any concentration used in the assays, demonstrating the dormant behavior of MBP in the factor Xa-cleaved rRbFerM fusion protein product.

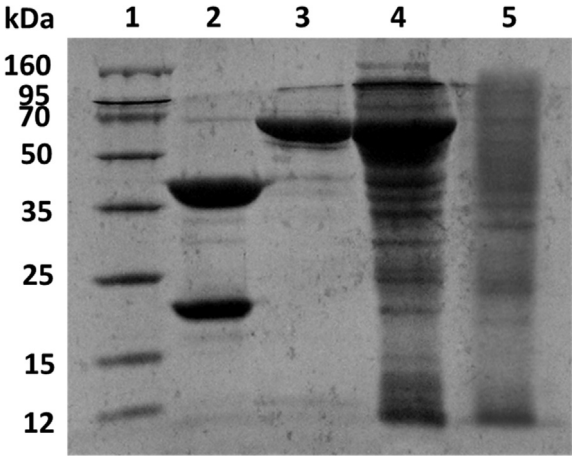

Fig. 4. SDS-PAGE analysis of the overexpressed and purified recombinant RbFerM fusion protein and cleaved products after treatment of the fusion protein with factor Xa. Lane 1, protein marker (Enzynomics, Korea); Lane 2, resultant cleaved products (MBP and rRbFerM) of the rRbFerM fusion protein after treatment with factor Xa; Lane 3, purified recombinant fusion protein (rRbFerM–MBP) after IPTG induction (1 mM); Lane 4, crude extract of rRbFerM after IPTG induction; Lane 5, total cellular extract from *E. coli* BL21 (DE3) carrying the rRbFerM–MBP expression vector prior to IPTG induction.

3.5. *Iron chelation activity of rRbFerM as a function of temperature*

Temperature dependence of the iron chelation activity of rRbFerM was investigated using 100 μg of the recombinant protein, following the same assay protocol implemented in the concentration-dependent experiment. The percentage of iron

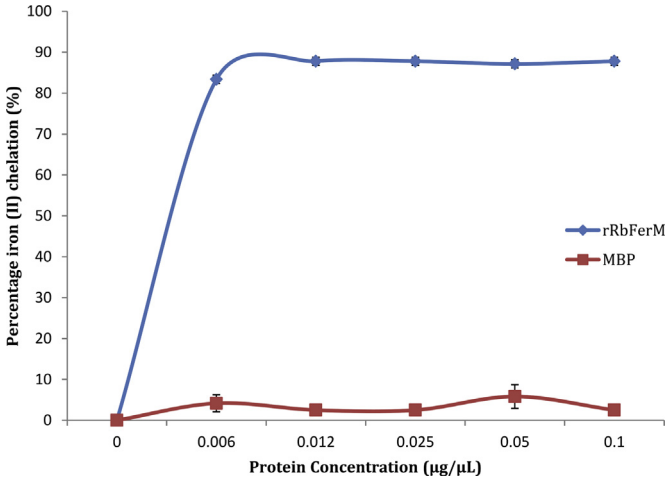

Fig. 5. *In vitro* iron chelation activity at different concentrations of rRbFerM. Error bars represent SDs ($n = 3$). Ferrozine was added and OD_{562} was measured after mixing $FeSO_4$ with different concentrations of rRbFerM, followed by incubation at room temperature for 10 min.

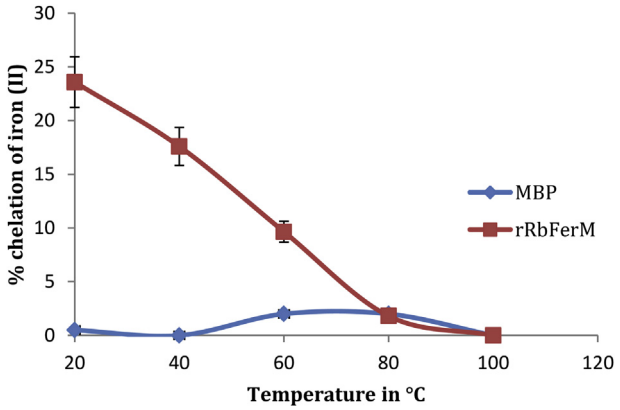

Fig. 6. Variation of *in vitro* iron chelation activity of rRbFerM with temperature. Error bars represent SDs ($n = 3$). Each assay was carried out with 0.05 μg/μL of rRbFerM.

chelation drastically declined as a result of increasing the temperature from 20 °C to 100 °C (Fig. 6), suggesting that heat may damage the three-dimensional folding of the protein, thereby alter the structure of its iron-binding sites. Interestingly, the reduction in iron chelation of rRbFerM with increasing temperature was found to be comparable with results of a previous study on the ferritin M subunit from *S. maximus*, in which the heat-denatured recombinant protein did not show any detectable iron chelation at any protein concentration used in the experiment [13]. Collectively, our observations with rRbFerM suggest that it can actively bind Fe (II) at lower temperatures, which are compatible with the natural environmental conditions of rock bream. MBP did not show any considerable iron chelation at any temperature, affirming its negligible interference with the iron-withholding function of rRbFerM.

3.6. DNA protection effect of rRbFerM under oxidative stress

Iron (II) ions can form hydroxyl radicals through Fenton-type reactions as a result of interactions with the H_2O_2 yielded in cellular metabolic processes, which render DNA damage in cells [40]. However, ferritins can potentially chelate these ions and can thus prevent the occurrence of Fenton-type reactions while protecting DNA from oxidative damage. Accordingly, rRbFerM demonstrated detectable protection against iron (II)- and H_2O_2-mediated DNA damage. As shown in Fig. 7, strand cleavage of pUC19 DNA was significantly inhibited in rRbFerM-treated reaction mixtures. Furthermore, as expected, the suppression of DNA breakage

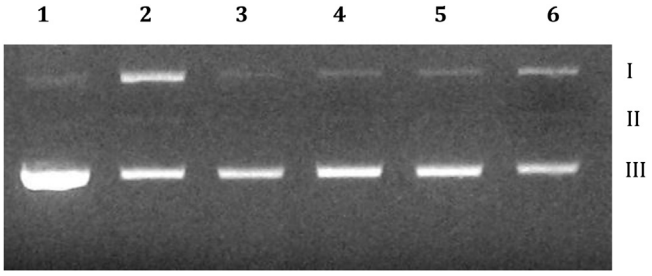

Fig. 7. The effect of rRbFerM on DNA cleavage by reaction of H_2O_2 with iron (II) ions, as analyzed using agarose gel electrophoresis. I, II, III represent the circular, linear and supercoiled plasmid conformations, respectively. Lane 1, pUC19 plasmid DNA alone; Lane 2, reaction mixture without the addition of rRbFerM (untreated); Lane 3, reaction mixture treated with 100 μg of rRbFerM; Lane 4, reaction mixture treated with 50 μg of rRbFerM; Lane 5, reaction mixture treated with 25 μg of rRbFerM; Lane 6, reaction mixture treated with 100 μg of MBP.

was detected to be more prominent with increasing concentrations of rRbFerM. In contrast, untreated and MBP-treated controls did not show any significant protection effect on pUC19 DNA cleavage rendered by iron (II) and the H_2O_2 system, as evidenced by a prominent band in the gel corresponding with the nicked form of the vector. However, compared to the untreated control, the DNA band corresponding to the nicked form of the vector in MBP-treated control was appeared to be less intense, probably due to the potential physical interference of MBP on the radical generating reaction between iron (II) and H_2O_2, since addition of MBP (~42.5 kDa) like bulk protein into the reaction medium can reduce the mobility as well as the probability of collision of the reactants while bringing down the reaction rate within a given period of time. Collectively, our observations affirm that RbFerM can act as an inhibitor of cellular DNA damage probably due to its iron sequestrating function, further providing indirect evidence of its potent antioxidant properties.

3.7. Transcriptional distribution of RbFerM in selected tissues

The q-PCR analysis revealed that RbFerM was ubiquitously transcribed in tissues of healthy fish. The most prominent mRNA expression level was detected in blood cells, and moderately high expression levels were observed in liver, heart, and brain tissues, compared to the level in the head kidney (Fig. 8). Ferritins are considered as iron storing molecules owing to the iron nucleation function of their L subunits [41], and they are known to act as acute phase proteins that are involved in several inflammatory reactions [42]. Furthermore, through its iron-withholding strategy, ferritin functions as an antimicrobial protein by suppressing bacterial proliferation in host cells and reducing the free iron ion availability for bacterial growth [43]. These properties likely explain the fact that the most pronounced transcript level of RbFerM was observed in the blood, which is another characteristic feature of L and H subunits; this is because blood cells, especially macrophages, can store iron after erythrophagocytosis and release it under thorough regulation of proteins involved in iron metabolism, such as ferritins [44,45]. Moreover, blood cells are involved in the innate immune system and play a key role in forming an organism's first line of defense against infection. Severe susceptibility to invading pathogens requires frequent immune responses against foreign invaders, thereby enhancing the basal metabolism of the blood cells involved in the immune response. As a consequence, generation of reactive oxygen species (ROS) such as H_2O_2 increases, which in turn induces the basal expression of ferritin-like iron sequestrating molecules to suppress Fenton-type reactions and prevent further free radical generation [1]. The liver is considered to be a long term iron reservoir [46], probably because of its substantial composition of L ferritins. The brain and heart are known to be enriched with H ferritins [46], which may be directly involved in iron metabolism through their ferroxidase activities. Accordingly, we observed moderately high transcript levels in the liver, brain, and heart. On the other hand, liver, brain and heart are known to be highly vascularized organs, there by prominent ferritin M expression in tissues in those organs are likely to be expected due to its most pronounced expression in blood.

Ref. [28] showed that the ferritin M-like subunit from *S. ocellatus* also exhibited a constitutive transcriptional profile in tissues examined, in which more pronounced expression levels were detected in the blood and liver, consistent with our observation regarding RbFerM. In *S. ocellatus*, ferritin M expression was found to be relatively low in the brain and heart compared to the lowest transcript level that was detected in the gill. In contrast, transcript levels of ferritin M from *S. maximus* were found to be most abundant in the muscle and spleen [13], whereas ferritin M from *C.*

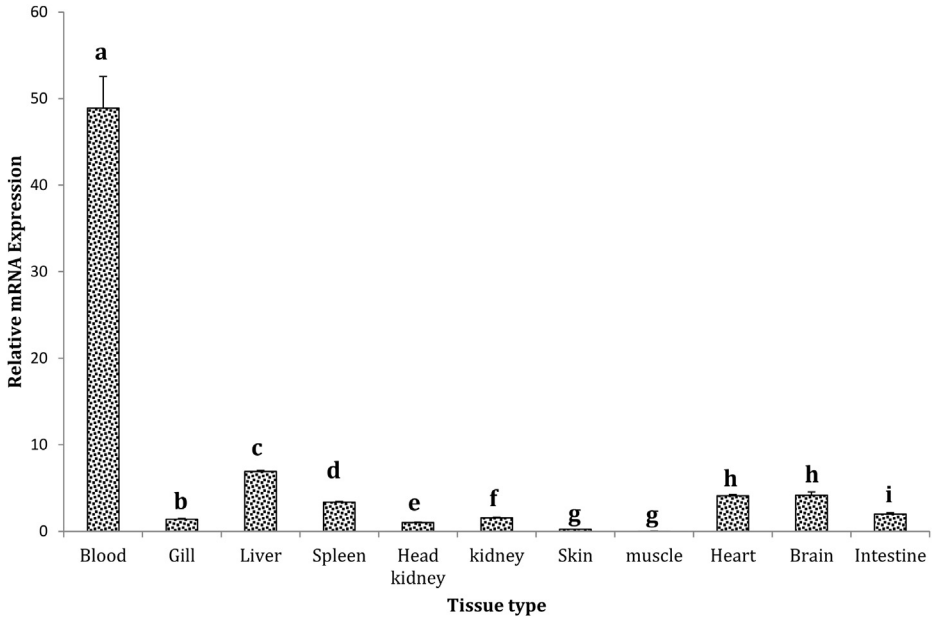

Fig. 8. The transcriptional distribution of RbFerM among different tissues of rock bream determined by q-PCR. Fold changes in expression are shown relative to the mRNA expression level in the head kidney. Error bars represent SDs ($n = 3$). Bars with different letters are significantly different ($P < 0.05$) from each other.

semilaevis was found to be most prominently expressed in the liver [26]. Moreover, the ferritin M subunit identified from *P. crocea* was highly expressed in the liver and muscle tissues [27]. Surprisingly, another ortholog of the ferritin M subunit characterized from *S. salar* was found to be exclusively transcribed in gonads, which provided a remarkable breakthrough regarding ferritin M expression under physiological conditions in teleosts [11].

3.8. Transcriptional behavior of RbFerM upon immune stimulation

In order to anticipate the immunological behavior of RbFerM in rock bream upon pathogen infection, its temporal transcriptional modulation in the liver was investigated under pathological conditions by using 3 live pathogens, *E. tarda*, *S. iniae*, and RBIV, along with the well-characterized bacterial endotoxin LPS for immune stimulation. The results showed that bacterial and viral stimuli significantly enhanced RbFerM transcription ($P < 0.05$) in liver tissues, suggesting its potential involvement in host immune defense and confirming documented evidence of its expressional modulation upon microbial infection [47,48]. As shown in Fig. 9A, upon LPS stimulation, the RbFerM transcript level was significantly elevated ($P < 0.05$), exhibiting an approximately 5-fold increase compared to the basal level. However, the expression level subsequently dropped down to the basal level at 6 h post-injection (p.i) and did not show any detectable upregulation throughout the remainder of the experiment. Similarly, pathogenic stress due to *E. tarda* also significantly upregulated RbFerM transcription levels ($P < 0.05$), demonstrating the highest fold expression (~2.5-fold) at 3 h p.i (Fig. 9B), and even further augmenting the expression level at 6 h p.i. Because LPS is a well-characterized endotoxin of Gram-negative bacteria such as *E. tarda*, the compatible transcriptional modulation patterns detected in LPS and *E. tarda* challenges at the early phase of the experiment might be attributed to the activation of the same immune signaling pathway. Nevertheless, upon *E. tarda* exposure, RbFerM transcription was significantly downregulated at the late phase of the experiment (12 h and 24 h p.i; $P < 0.05$), showing a deviation in the expressional profile compared to that under LPS exposure. This observation can be attributed to the nature of the stimulant in these challenge experiments because, as a live pathogen, *E. tarda* may exert different and specific evasion mechanisms in rock bream against host immune mechanisms, as has been demonstrated in several bacterial species [49].

As previously reported, the mRNA expression level of the *S. ocellatus* ferritin M subunit in the liver was found to be upregulated by *E. tarda* infection from 4 to 48 h p.i, eliciting both early- and late-phase inductions [28]. However, upon stimulation of Gram-negative bacteria such as *Listonella anguillarum*, ferritin M transcription was induced at the late phase of the experiment (12 h, 24 h, and 48 h) in the liver and spleen tissues of *S. maximus* [13], whereas in *C. semilaevis*, this induction occurred only at the early phase of the experiment in the liver (1 h and 4 h) and spleen (4 h), but in both phases of the experiment in the kidney (1 h, 4 h, 24 h, 48 h) [26]. Moreover, in *P. crocea*, the ferritin M transcript level in the kidney was markedly elevated 5 days after stimulation, whereas it reached its maximum expression at 12 h p.i in both the spleen and liver [27].

Under the pathogenic stress evoked by the Gram-positive bacteria *S. iniae*, RbFerM transcription was also significantly upregulated in the liver at both 3 h (~2.5 fold) and 6 h (~4 fold) p.i, which resembled the early-phase response upon *E. tarda* exposure (Fig. 9C). However, at 12 h p.i, the RbFerM transcript level was detected to be almost equal to the basal level, where it was maintained throughout the rest of the experiment. As mentioned earlier, ferritins are known to involve in acute phase reactions through its intracellular iron sequestrating and storage abilities triggering immune responses [50]. They play crucial roles in protecting the organisms against microbial proliferation in host cells and oxidative damage [1,43]. Therefore, the detected inductive expression of RbFerM upon the stimulation of *S. iniae* may reflect its potential acute phase engagement in bacteriostatic strategy of host defense. On the other hand it possibly arose in order to counterbalance the production of ROS upon bacterial invasion, through sequestrating the Fe (II) ions, since pathogen infections prompt the ROS production as a primary defensive mechanism functioning in host phagocytic cells [51]. According to the transcriptional profile

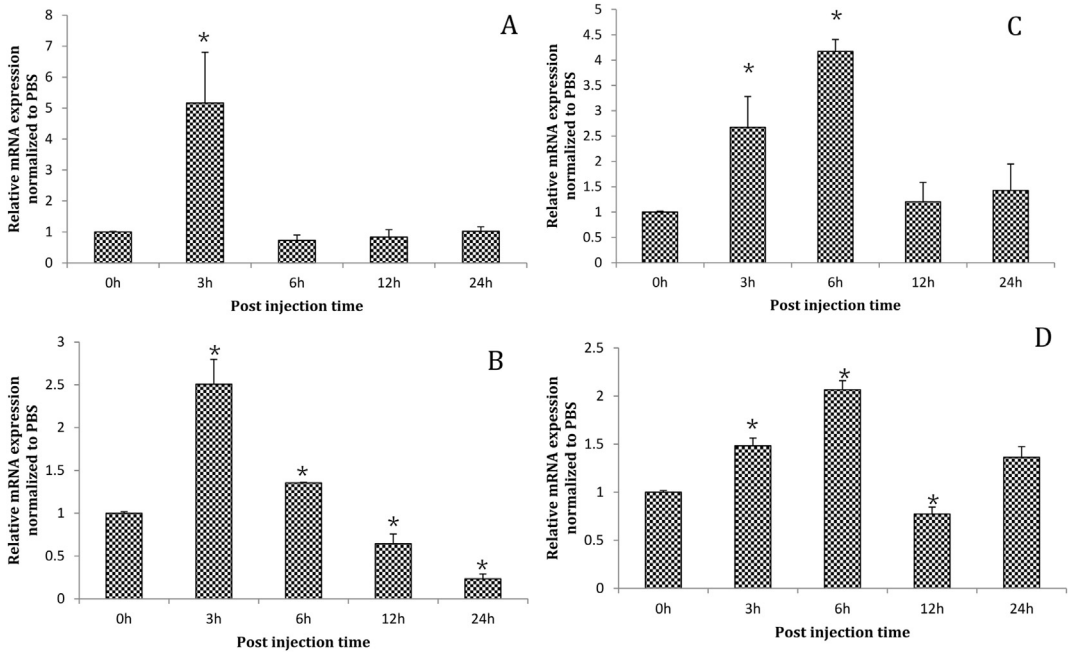

Fig. 9. Expression profile of RbFerM mRNA in liver tissues upon immune stimulation with (A) LPS, (B) *E. tarda*, (C) *S. iniae*, (D) RBIV, as determined by q-PCR. The relative expression was calculated by the $2^{-\Delta\Delta CT}$ method by using rock bream β-actin as the reference gene with respect to corresponding PBS-injected controls at each time point. The relative fold change in expression at 0 h post-injection was used as the basal line. Error bars represent SDs ($n = 3$); $^{*}P < 0.05$.

observed in liver and kidney tissues of *C. semilaevis* after challenge with *S. iniae*, ferritin M transcription was elevated at the early phase (4 h) and the late phase (24 h), while inductive responses were observed exclusively at the late phase (24 h and 48 h p.i) in kidney tissues [26]. Furthermore, the same stimulant significantly upregulated the mRNA expression level of the *S. ocellatus* ferritin M subunit from 4 to 48 h p.i in the liver tissues ($P < 0.05$ and $P < 0.01$), while elevating M ferritin transcription in the liver and spleen from 12 to 48 h and from 8 to 48 h, respectively.

This study provides the first report of transcriptional modulation of the ferritin M subunit upon live virus infection in a teleost species, rock bream. q-PCR analysis revealed that the RbFerM transcript level was significantly induced by RBIV exposure at the early phase of the experiment (3 h and 6 h p.i; $P < 0.05$), reaching the highest expression level (~2-fold) at 6 h p.i (Fig. 9D). However, at 12 h p.i, significant downregulation of RbFerM expression was observed ($P < 0.05$), either as a response to viral evasion mechanisms orchestrated against the host immune defense [52] or because of the influence of the virus' induction of ROS production in host cells in order to propagate its infection into other cells [53] because ferritins can suppress ROS production through inhibition of Fenton-type reactions by sequestrating free iron in cellular environments [54]. Even though, to our knowledge, no studies have addressed expressional inductions of ferritin M subunits upon live viral pathogen infections in teleosts, one study on *S. maximus* provides some evidence about this process, in which a viral mitogen, poly I:C, was used to stimulate fish instead of a live virus, and it was found to substantially enhance transcription of the ferritin M subunit in the liver and spleen tissues compared to controls [13]. The overall inductive response of RbFerM upon different pathogen and mitogen stimuli observed in the present study suggests its potential role in host immune defense, which further confirms the results of a previous study on the antimicrobial behavior of ferritins through its iron depriving function [43]. However, since the experimental fish were kept under identical conditions in tanks throughout the whole experimentation in all of the challenge experiments, the stress responses elicited by fish may be interfered by the tank effect to a certain extent, especially due to the back ground color (herein blue color) and limited space of the tanks, compared to its natural habitat.

4. Conclusion

Overall molecular insight into RbFerM provides strong evidence pointing to its importance as a subunit of the rock bream ferritin protein complex, which resembles structural features of ferritin H and L subunits, especially those involved in iron chelation. Moreover, through its iron depriving properties, RbFerM can provide a protective effect against potential DNA damage, which is most likely induced by hydroxyl radicals generated through Fenton-type reactions. Iron-binding properties of RbFerM can vary as a function of temperature, and it exhibits optimal activity under the physiological temperature of rock bream. Phylogenetic analysis confirmed that RbFerM evolved from a common ancestor origin of vertebrates. According to the modulated transcriptional profile upon pathogen stimulation, RbFerM expression appears to be promoted under viral and bacterial stress, further demonstrating its potential role in the host immune defense, which is likely based on the reduction of free iron availability resulting from its iron-withholding effect.

Acknowledgments

This research was supported by National Fisheries Research and Development Institute (RP-2013-BT-059).

References

[1] Orino K, Lehman L, Tsuji Y, Ayaki H, Torti SV, Torti FM. Ferritin and the response to oxidative stress. Biochem J 2001;357:241–7.
[2] Watt RK. The many faces of the octahedral ferritin protein. Biometals 2011;24:489–500.
[3] Crichton RR, Declercq JP. X-ray structures of ferritins and related proteins. Biochim Biophys Acta 2010;1800:706–18.

[4] Arosio P, Ingrassia R, Cavadini P. Ferritins: a family of molecules for iron storage, antioxidation and more. Biochim Biophys Acta 2009;1790:589–99.
[5] Caskey JH, Jones C, Miller YE, Seligman PA. Human ferritin gene is assigned to chromosome 19. Proc Natl Acad Sci U S A 1983;80:482–6.
[6] Worwood M, Brook JD, Cragg SJ, Hellkuhl B, Jones BM, Perera P, et al. Assignment of human ferritin genes to chromosomes 11 and 19q13.3––19qter. Hum Genet 1985;69:371–4.
[7] Lawson DM, Artymiuk PJ, Yewdall SJ, Smith JM, Livingstone JC, Treffry A, et al. Solving the structure of human H ferritin by genetically engineering intermolecular crystal contacts. Nature 1991;349:541–4.
[8] Santambrogio P, Levi S, Cozzi A, Corsi B, Arosio P. Evidence that the specificity of iron incorporation into homopolymers of human ferritin L- and H-chains is conferred by the nucleation and ferroxidase centres. Biochem J 1996;314(Pt 1):139–44.
[9] Arosio P, Yokota M, Drysdale JW. Structural and immunological relationships of isoferritins in normal and malignant cells. Cancer Res 1976;36:1735–9.
[10] Lawson DM, Treffry A, Artymiuk PJ, Harrison PM, Yewdall SJ, Luzzago A, et al. Identification of the ferroxidase centre in ferritin. FEBS Lett 1989;254:207–10.
[11] Andersen O, Dehli A, Standal H, Giskegjerde TA, Karstensen R, Rorvik KA. Two ferritin subunits of Atlantic salmon (*Salmo salar*): cloning of the liver cDNAs and antibody preparation. Mol Mar Biol Biotechnol 1995;4:164–70.
[12] Dickey LF, Sreedharan S, Theil EC, Didsbury JR, Wang YH, Kaufman RE. Differences in the regulation of messenger RNA for housekeeping and specialized-cell ferritin. A comparison of three distinct ferritin complementary DNAs, the corresponding subunits, and identification of the first processed in amphibia. J Biol Chem 1987;262:7901–7.
[13] Zheng WJ, Hu YH, Sun L. Identification and analysis of a *Scophthalmus maximus* ferritin that is regulated at transcription level by oxidative stress and bacterial infection. Comp Biochem Physiol B Biochem Mol Biol 2010;156:222–8.
[14] Wang W, Knovich MA, Coffman LG, Torti FM, Torti SV. Serum ferritin: past, present and future. Biochim Biophys Acta 2010;1800:760–9.
[15] Alkhateeb AA, Connor JR. Nuclear ferritin: a new role for ferritin in cell biology. Biochim Biophys Acta 2010;1800:793–7.
[16] Coffman LG, Brown JC, Johnson DA, Parthasarathy N, D'Agostino Jr RB, Lively MO, et al. Cleavage of high-molecular-weight kininogen by elastase and tryptase is inhibited by ferritin. Am J Physiol Lung Cell Mol Physiol 2008;294:L505–15.
[17] Parthasarathy N, Torti SV, Torti FM. Ferritin binds to light chain of human H-kininogen and inhibits kallikrein-mediated bradykinin release. Biochem J 2002;365:279–86.
[18] Torti SV, Kwak EL, Miller SC, Miller LL, Ringold GM, Myambo KB, et al. The molecular cloning and characterization of murine ferritin heavy chain, a tumor necrosis factor-inducible gene. J Biol Chem 1988;263:12638–44.
[19] Torti FM, Torti SV. Regulation of ferritin genes and protein. Blood 2002;99:3505–16.
[20] Outten FW, Theil EC. Iron-based redox switches in biology. Antioxid Redox Signal 2009;11:1029–46.
[21] Theil EC. Coordinating responses to iron and oxygen stress with DNA and mRNA promoters: the ferritin story. Biometals 2007;20:513–21.
[22] Wu C, Zhang W, Mai K, Xu W, Wang X, Ma H, et al. Transcriptional up-regulation of a novel ferritin homolog in abalone *Haliotis discus hannai* Ino by dietary iron. Comp Biochem Physiol C Toxicol Pharmacol 2010;152:424–32.
[23] Zhou J, Wang W, Ma G, Wang A, He W, Wang P, et al. Gene expression of ferritin in tissue of the Pacific white shrimp, *Litopenaeus vannamei* after exposure to pH stress. Aquaculture 2008;275:356–60.
[24] Salinas-Clarot K, Gutierrez AP, Nunez-Acuna G, Gallardo-Escarate C. Molecular characterization and gene expression of ferritin in red abalone (*Haliotis rufescens*). Fish Shellfish Immunol 2011;30:430–3.
[25] Theil EC. Ferritin: structure, gene regulation, and cellular function in animals, plants, and microorganisms. Annu Rev Biochem 1987;56:289–315.
[26] Wang W, Zhang M, Sun L. Ferritin M of *Cynoglossus semilaevis*: an iron-binding protein and a broad-spectrum antimicrobial that depends on the integrity of the ferroxidase center and nucleation center for biological activity. Fish Shellfish Immunol 2011;31:269–74.
[27] Zhang X, Wei W, Wu H, Xu H, Chang K, Zhang Y. Gene cloning and characterization of ferritin H and M subunits from large yellow croaker (*Pseudosciaena crocea*). Fish Shellfish Immunol 2010;28:735–42.
[28] Hu YH, Zheng WJ, Sun L. Identification and molecular analysis of a ferritin subunit from red drum (*Sciaenops ocellatus*). Fish Shellfish Immunol 2010;28:678–86.
[29] Zenke K, Kim KH. Functional characterization of the RNase III gene of rock bream iridovirus. Arch Virol 2008;153:1651–6.
[30] Park SL. Disease control in Korean aquaculture. Fish Pathol 2006;44:19–23.
[31] Whang I, Lee Y, Kim H, Jung SJ, Oh MJ, Choi CY, et al. Characterization and expression analysis of the myeloid differentiation factor 88 (MyD88) in rock bream *Oplegnathus fasciatus*. Mol Biol Rep 2011;38:3911–20.
[32] Tamura K, Dudley J, Nei M, Kumar S. MEGA4: molecular evolutionary genetics analysis (MEGA) software version 4.0. Mol Biol Evol 2007;24:1596–9.
[33] Umasuthan N, Whang I, Kim JO, Oh MJ, Jung SJ, Choi CY, et al. Rock bream (*Oplegnathus fasciatus*) serpin, protease nexin-1: transcriptional analysis and characterization of its antiprotease and anticoagulant activities. Dev Comp Immunol 2011;35:785–98.
[34] Bradford MM. A rapid and sensitive method for the quantitation of microgram quantities of protein utilizing the principle of protein-dye binding. Anal Biochem 1976;72:248–54.
[35] De Zoysa M, Lee J. Two ferritin subunits from disk abalone (*Haliotis discus discus*): cloning, characterization and expression analysis. Fish Shellfish Immunol 2007;23:624–35.
[36] Kang JH. Oxidative damage of DNA induced by ferritin and hydrogen peroxide. Bull Korean Chem Soc 2010;31:2873–6.
[37] Whang I, Lee Y, Lee S, Oh MJ, Jung SJ, Choi CY, et al. Characterization and expression analysis of a goose-type lysozyme from the rock bream *Oplegnathus fasciatus*, and antimicrobial activity of its recombinant protein. Fish Shellfish Immunol 2011;30:532–42.
[38] Livak KJ, Schmittgen TD. Analysis of relative gene expression data using real-time quantitative PCR and the 2(−Delta Delta C(T)) method. Methods 2001;25:402–8.
[39] Thomson AM, Rogers JT, Leedman PJ. Iron-regulatory proteins, iron-responsive elements and ferritin mRNA translation. Int J Biochem Cell Biol 1999;31:1139–52.
[40] Luo Y, Henle ES, Linn S. Oxidative damage to DNA constituents by iron-mediated fenton reactions. The deoxycytidine family. J Biol Chem 1996;271:21167–76.
[41] Thompson KJ, Fried MG, Ye Z, Boyer P, Connor JR. Regulation, mechanisms and proposed function of ferritin translocation to cell nuclei. J Cell Sci 2002;115:2165–77.
[42] Worwood M. Ferritin. Blood Rev 1990;4:259–69.
[43] Ong ST, Ho JZ, Ho B, Ding JL. Iron-withholding strategy in innate immunity. Immunobiology 2006;211:295–314.
[44] Knutson MD, Oukka M, Koss LM, Aydemir F, Wessling-Resnick M. Iron release from macrophages after erythrophagocytosis is up-regulated by ferroportin 1 overexpression and down-regulated by hepcidin. Proc Natl Acad Sci U S A 2005;102:1324–8.
[45] Hausmann K, Wulfhekel U, Dullmann J, Kuse R. Iron storage in macrophages and endothelial cells. Histochemistry, ultrastructure, and clinical significance. Blut 1976;32:289–95.
[46] Harrison PM, Arosio P. The ferritins: molecular properties, iron storage function and cellular regulation. Biochim Biophys Acta 1996;1275:161–203.
[47] Orino K, Watanabe K. Molecular, physiological and clinical aspects of the iron storage protein ferritin. Vet J 2008;178:191–201.
[48] Knovich MA, Storey JA, Coffman LG, Torti SV, Torti FM. Ferritin for the clinician. Blood Rev 2009;23:95–104.
[49] Pieters J. Evasion of host cell defense mechanisms by pathogenic bacteria. Curr Opin Immunol 2001;13:37–44.
[50] Weiss G, Goodnough LT. Anemia of chronic disease. N Engl J Med 2005;352:1011–23.
[51] Babior BM. The respiratory burst of phagocytes. J Clin Invest 1984;73:599–601.
[52] Iannello A, Debbeche O, Martin E, Attalah LH, Samarani S, Ahmad A. Viral strategies for evading antiviral cellular immune responses of the host. J Leukoc Biol 2006;79:16–35.
[53] Spooner R, Yilmaz O. The role of reactive-oxygen-species in microbial persistence and inflammation. Int J Mol Sci 2011;12:334–52.
[54] Berberat PO, Katori M, Kaczmarek E, Anselmo D, Lassman C, Ke B, et al. Heavy chain ferritin acts as an antiapoptotic gene that protects livers from ischemia reperfusion injury. FASEB J 2003;17:1724–6.